Reviews on Advanced Materials and Technologies, 2026, vol. 8, no. 2, pp. 81–86
DOI: 10.17586/2687-0568-2026-8-2-81-86

Anisotropy and Strain Energy in Decahedral Particles

A.M. Smirnov [1], R.E. Shevchuk [1,2], S.A. Krasnitckii [1], A.E. Romanov [1,3]

[1] ITMO University, Kronverkskiy pr., 49, bldg. A, St. Petersburg, 197101, Russia
[2] Baltic State Technical University «VOENMEH» named after D.F. Ustinov, 1st Krasnoarmeyskaya st. 1, St. Petersburg, 190005, Russia
[3] Ioffe Institute, Polytekhnicheskaya st. 26, St. Petersburg, 194021, Russia

Article history

Received March 25, 2026
Accepted May 05, 2026
Available online May 12, 2026

Abstract

This study analyzes the strain energy stored in decahedral particles through finite-element (FE) simulations that fully account for material anisotropy. The particle is modeled as an assembly of five perfect tetrahedra with a geometrically necessary gap. A two-stage FE procedure is employed: first, prescribed displacements close the gap to generate the eigenstrain; second, the resulting stress-strain state is calculated as the elastic response arising from the introduced eigenstrain. To quantify the influence of anisotropy on the particle strain energy, we introduce an anisotropy coefficient, defined in terms of the engineering elastic constants. The numerical results are compared with isotropic analytical models based on Voigt, Reuss, and Hill homogenization schemes for a range of face-centered cubic metals. We demonstrate that isotropic approximations consistently overestimate the strain energy, the Reuss scheme provides the closest agreement to the FE solution (deviations below 26% even for highly anisotropic Pb). For weakly anisotropic materials such as Al, the considered schemes yield similar inaccuracy of approximately 8%. Our findings underscore the necessity of incorporating material anisotropy for accurate quantitative predictions of strain energy in decahedral particles.

Keywords: Finite-element method; Strain energy; Disclinations; Decahedral particles

1. INTRODUCTION

The widespread application of face-centered cubic (FCC) metallic decahedral nanoparticles (DhPs) in plasmonics and catalysis stems directly from their unique structural characteristics [1,2]. In plasmonics, the anisotropy of DhPs supports two distinct dipolar plasmon resonance modes: azimuthal (oscillations in the equatorial plane of DhP) and polar (oscillations along the direction of the fivefold rotational axis) [3]. With increasing DhP size (above 65 nm), a quadrupole mode emerges, and the intensity of this mode rises with particle size [4]. The anisotropy of DhPs defined multiple plasmon modes which are widely exploited to broaden the spectral range of the particle's response, generate stronger localized fields, and enhance the efficiency of light absorption. In catalysis, DhP twin boundaries and surface facets provide a high density of active sites, making them exceptionally efficient for both optical and chemical transformations [5,6]. For instance, Pd pentagonal nanoparticles significantly stimulate the higher activity towards electrochemical reduction of CO_2 in comparison with Pd octahedrons [7]. Besides, Pt-DhPs are successfully utilized in the oxygen reduction reaction [8]. Thus, most studies recognize that the unique properties of DhPs are attributed to their anisotropy and structure.

In terms of the particle structure, DhPs consist of five tetrahedral single-crystal domains sharing a fivefold twinning axis. The tetrahedra are bounded by {111}-type facets, with edges oriented along <110>-type crystallographic directions [9]. This crystallographic configuration creates an angular deficit between the tetrahedral ($\omega \approx 0.128$ rad or 7.35°), resulting in elastic strain. It is well known that this strain affects not only the thermodynamic stability of DhPs but also their electronic structure and catalytic activity. Hence, the accurate modeling of the strain-stress state is crucial for the rational design of DhP based materials.

* Corresponding author: A.M. Smirnov, e-mail: smirnov.mech@gmail.com

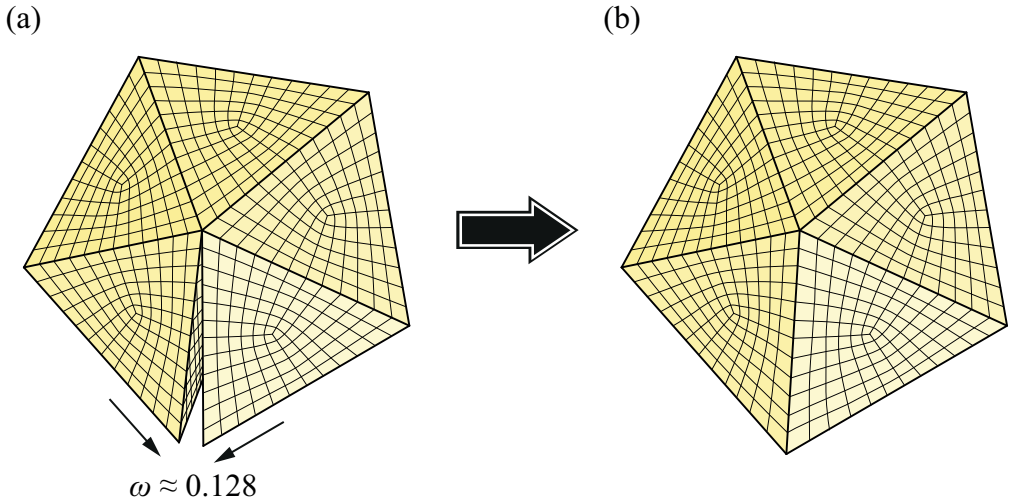

Fig. 1. FE model of a DhP with FE mesh: (a) geometry used for the first stage (simulating gap closure); (b) geometry used for the second stage (calculating the stress-strain state).

The most proper analytical model for describing the strain energy of a DhP is credited to Polonsky et al. [10,11]. In this model, the particle is approximated as an elastic sphere with a disclination at its center. The Polonsky model provides valuable analytical insight, however this model based on the isotropic assumption ignores the crystallographic anisotropy of the DhP. Consequently, the validity of its predictions for actual anisotropic particles remains unclear.

In the present study, we suggest a FE model of an anisotropic DhP that explicitly accounts for its crystallographic structure. Comparing systematically the results of anisotropic FE simulations with those of Polonsky isotropic model, we quantify the influence of anisotropy on the strain energy of the particles. This analysis establishes the limits of applicability of isotropic approximation and provides a more accurate framework for predicting the stress-strain state in DhPs, which is essential for understanding their stability and functional properties in plasmonic and catalytic applications.

2. MODEL

We consider the FE approach to calculate the strain energy of decahedral particles. This approach is similar to the disclination one [12]. The key advantage of the FE method lies in its ability to consider the specific geometric features (such as faceting) and material anisotropy via numerical solution of the governing equations.

Fig. 1 shows the FE model of a DhP with FE mesh. The problem is solved in two stages. In the first stage (Fig. 1a), a gap is closed; this gap is geometrically necessary for the assembly of five ideal tetrahedra. It should be noted that the elastic constants C_{11}, C_{12}, and C_{44} (typical for FCC materials) are assigned for each tetrahedron. This assignment considers the crystallographic orientation of each individual tetrahedron with respect to the global coordinate system. The gap is closed by applying prescribed displacements to the mesh nodes located on its surfaces. Once the gap boundaries are closed, the DhP acquires an eigenstrain equivalent to a wedge disclination at its center. The second stage (Fig. 1b) involves computing the stress-strain state as the elastic response arising from the introduced eigenstrain. Thus, the total displacement, strain, and stress fields of the DhP are computed numerically, with material anisotropy taken into consideration.

A detailed description of the calculation procedure can be found in our recent paper [13].

3. RESULTS AND DISCUSSION

To analyze the effect of anisotropy on the strain energy of the DhP, it is convenient to use the anisotropy coefficient A, which is determined through the engineering anisotropic elastic constants in following form [14]:

$$A = \frac{2(1+\nu^{eng})G^{eng}}{E^{eng}}, \tag{1}$$

where E^{eng}, G^{eng} and ν^{eng} are engineering Young modulus, shear modulus and Poisson ratio respectively.

Note that the engineering constants E^{eng}, G^{eng} and ν^{eng} are related to the elastic constants C_{ij} for a cubic material in Voigt notation as follows:

$$E^{eng} = \frac{(C_{11}-C_{12})(C_{11}+2C_{12})}{C_{11}+C_{12}} \text{ along a <100> direction,} \tag{2}$$

$$G^{eng} = C_{44} \text{ shear on a \{100\} plane in the <010> direction,} \tag{3}$$

$$\nu^{eng} = \frac{C_{12}}{C_{11}+C_{12}} \text{ for tension along <100> and lateral strain along <010> direction.} \tag{4}$$

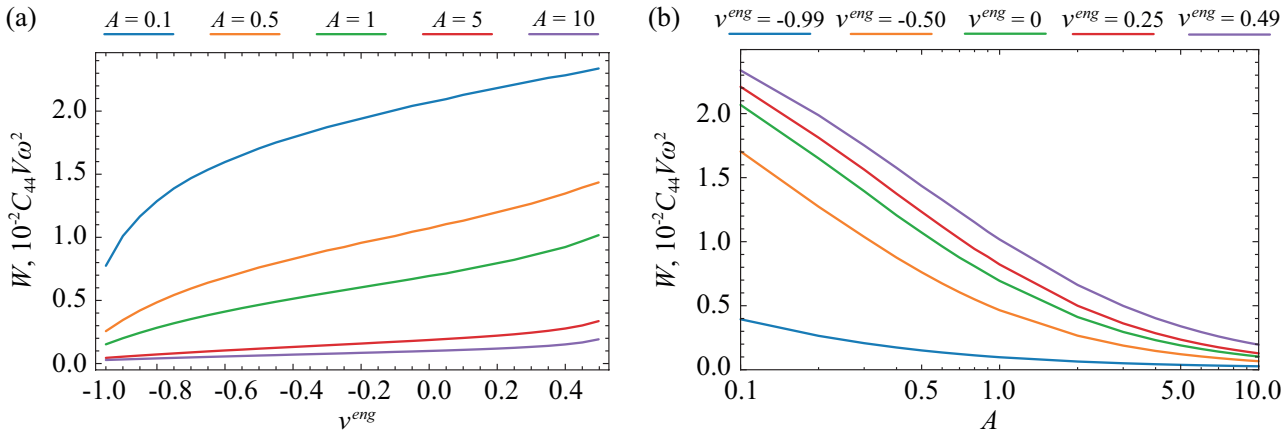

Fig. 2. Strain energy of an anisotropic DhP. Dependence of the strain energy of DhP W (in units of $10^{-2}C_{44}V\omega^2$, where V is the decahedron volume) on changes in: (a) the engineering Poisson ratio ν^{eng} and (b) the anisotropy coefficient A.

The isotropic constants E, G and ν may be obtained by averaging the elastic constants C_{ij} according to the Voigt [15], Reuss [16] or Hill [17] methods:

$$G_V = \frac{C_{11} - C_{12} + 3C_{44}}{5}, \quad G_R = \frac{5C_{44}(C_{11} - C_{12})}{4C_{44} + 3(C_{11} - C_{12})},$$

$$G_H = \frac{G_V + G_R}{2}, \tag{5}$$

$$E_i = \frac{9KG_i}{3K + G_i}, \quad \nu_i = \frac{3K - 2G_i}{6K + 2G_i}, \; i = V, R, \text{ or } H, \tag{6}$$

$$K = \frac{C_{11} + 2C_{12}}{3}. \tag{7}$$

Figure 2 illustrates the combined influence of the engineering Poisson ratio ν^{eng}, and the anisotropy coefficient A on the strain energy W that is given in units of $10^{-2}C_{44}V\omega^2$ (V is the decahedron volume). As shown in Fig. 2a, for a fixed anisotropy coefficient A, the strain energy W decreases monotonically with a decrease in the engineering Poisson ratio ν^{eng}. Figure 2b shows the strong dependence of the strain energy W on the anisotropy coefficient A: for any given ν^{eng}, W is highest in weakly anisotropic materials and drops markedly as A increases. At high anisotropy levels ($A > 5$), the sensitivity of W to ν^{eng} diminishes, with curves for different ν^{eng} values nearly overlapping. This indicates that in strongly anisotropic materials, the anisotropy of the engineering shear moduli G^{eng}, characterized by the anisotropy coefficient A, dominates the strain energy W, suppressing the role of the engineering Poisson ratio ν^{eng}.

To evaluate the effect of material anisotropy on the strain energy W of a DhP, we compare the numerical results with the Polonsky analytical model that described the strain energy W as stored by a wedge disclination in an elastic sphere of volume V_{sp} as follows [10]:

$$W = \frac{3GV_{sp}}{1-\nu}\left(\frac{\omega}{2\pi}\right)^2\left[\frac{1}{12} - \frac{\nu(1+3\nu)}{15(7+5\nu)}\right.$$

$$\left. - \sum_{m=2}^{+\infty}\left\{\frac{(1+4m)(32m^4\nu^2 - 8m^3(\nu^2 - 7\nu + 1) - 4m^2(1-\nu)}{4(m-1)m(2m-1)(3+8m+4m^2)^2(1+\nu+2m+4m^2+2m\nu)}\right.\right.$$

$$\left.\left. + \frac{2m(11\nu^2 - 7\nu - 9) - (1+\nu)(5-4\nu))}{4(m-1)m(2m-1)(3+8m+4m^2)^2(1+\nu+2m+4m^2+2m\nu)}\right\}\right]. \tag{8}$$

Table 1 presents a comparative analysis of the strain energy density W/V (in eV/nm^3 units) for DhPs in various FCC metals. The results obtained from the anisotropic FE analysis are compared against the isotropic analytical solutions (see Eq. (8)) based on homogenized mechanical properties. The homogenization was performed using three classical schemes: Voigt (uniform strain assumption), Reuss (uniform stress assumption), and Hill (arithmetic means of Voigt and Reuss), see Eq. (5)–(7). The elastic constants C_{11}, C_{12}, and C_{44} [18,19], and the coefficient of anisotropy A for each metal are also listed, as they define the single-crystal anisotropic behavior used as input for the numerical model.

The choice of the averaging scheme (Voigt, Reuss, or Hill) has a noticeable effect on the analytical energy prediction. As expected, the Reuss estimate consistently yields the lowest energy values, while the Voigt estimate provides the upper bound. The Hill average falls between the two. This trend is consistent across all metals, reflecting the inherent differences in the underlying assumptions of stress and strain uniformity.

A critical finding is that the anisotropic FE analysis predicts a lower strain energy density compared to all three isotropic analytical estimates for every metal examined, and is in agreement with other works, such as that by Patala et al. [20]. For example, in Cu, the FE result (2.795 eV/nm^3) is substantially lower than the Voigt (4.414 eV/nm^3), the Reuss (3.438 eV/nm^3), and the Hill (3.938 eV/nm^3) estimates. This systematic overestimation by the isotropic models suggests that explicitly accounting for crystallographic anisotropy is crucial for

Table 1. Comparison of the strain energy density W/V given in units of eV/nm^3 between isotropic analytical solutions with homogenized mechanical properties and anisotropic FE analysis for some FCC metals. The table also lists the elastic constants C_{ij} and the anisotropy coefficients A for the metals under consideration

Metal	Anisotropy coefficient A	Elastic constants C_{ij}, GPa			Analytical solution for W/V, eV/nm^3			FE solution for W/V, eV/nm^3
		C_{11}	C_{12}	C_{44}	Voigt	Reuss	Hill	
Al	1.21	114.3	61.9	31.6	0.870	0.864	0.867	0.805
Pt	1.48	358.1	253.5	77.5	5.267	5.148	5.164	4.477
Ni	2.39	261.2	150.8	131.7	11.330	9.877	10.680	8.666
Pd	2.46	234.2	176.1	71.2	3.777	3.232	3.508	2.687
Au	2.85	201.5	169.7	45.4	1.584	1.269	1.431	1.010
Ag	2.99	131.5	97.3	51.1	1.818	1.443	1.621	1.172
Cu	3.19	176.2	124.9	81.8	4.414	3.438	3.938	2.795
Pb	3.84	55.6	45.4	19.4	0.259	0.184	0.224	0.146

accurately capturing the elastic behavior of these pentagonal particles.

The Table 1 demonstrates that the strain energy density is highly sensitive to the specific metal. Materials with a high degree of elastic anisotropy (like Pb and Cu) show a larger spread between the Voigt and Reuss bounds, which in turn correlates with a more pronounced difference between the isotropic estimates and the anisotropic FE result. This indicates that the deviation from the isotropic approximation is directly linked to the material inherent anisotropy.

Since the FE solution accounts for material anisotropy, it should be more accurate than the analytical models. As shown in Table 1, the closest match to the FE results is provided by the Reuss averaging scheme. For this scheme, the difference does not exceed 26%, even for highly anisotropic Pb, while the Voigt scheme gives an error of 77%. For materials with low anisotropy, such as Al, all three averaging schemes yield a similar error of about 8%. These differences can be explained by the specific structure of the DhP. It has a distinguished <110>-type crystallographic direction along which the tetrahedral blocks are joined, making its symmetry close to that of a transversely isotropic body. Thus, to improve the accuracy of analytical predictions, the elastic constants of the cubic crystal should be recalculated for a transversely isotropic solid.

4. CONCLUSIONS

A two-stage FE procedure has been developed to model the stored strain energy in DhP. The method accounts for both the faceted geometry of the particle and the anisotropy of the crystal lattice. The anisotropy coefficient A has been introduced, expressed in terms of the engineering elastic constants. This coefficient provides a convenient measure for analyzing the influence of anisotropy on the strain energy W.

The strain energy W decreases monotonically with the decreasing engineering Poisson ratio ν^{eng} for a fixed anisotropy coefficient A. At high anisotropy levels ($A > 5$), the dependence on ν^{eng} becomes negligible, indicating that shear anisotropy dominates the elastic response.

Comparison of the FE results with isotropic analytical models based on Voigt, Reuss, and Hill averaging reveals that isotropic approximations systematically overestimate the strain energy. The Reuss scheme yields the closest match to the numerical solution, with deviations not exceeding 26% even for highly anisotropic Pb, whereas the Voigt scheme leads to errors as high as 77%. For materials with low anisotropy (e.g., Al), all three averaging schemes produce similar errors of approximately 8%, suggesting that the choice of homogenization method is less critical in such cases.

The observed differences are linked to the inherent symmetry of the DhP, which possesses a distinguished <110>-type crystallographic direction along which the tetrahedral blocks are joined. This makes the symmetry of the particle nearly transversely isotropic, implying that improved analytical estimates could be obtained by recalculating the cubic elastic constants for a transversely isotropic solid.

Finally, the results demonstrate that crystallographic anisotropy must be taken into account for reliable quantitative predictions of strain energy in DhPs. Isotropic homogenization techniques, while useful for qualitative estimates, are insufficient for accurate quantitative analysis.

ACKNOWLEDGEMENTS

This work was supported by the Russian Science Foundation (grant No. 23-72-10014).

REFERENCES

[1] S. Zhou, M. Zhao, T.-H. Yang, Y. Xia. Decahedral nanocrystals of noble metals: synthesis, characterization, and applications. *Mater. Today*, 2019, vol. 22, pp. 108–131.

[2] L.A. Sokura, A.M. Smirnov, A.E. Romanov. Chemical synthesis methods for controlling morphology and achieving uniform arrays of metal nanoparticles in semiconductor films. *Rev. Adv. Mater. Technol.*, 2025, vol. 7, no. 1, pp. 53–62.

[3] I. Pastoriza–Santos, A. Sánchez–Iglesias, F.J. García de Abajo, L.M. Liz–Marzán. Environmental optical sensitivity of gold nanodecahedra. *Adv. Funct. Mater.*, 2007, vol. 17, no. 9, pp. 1443–1450.

[4] J. Rodríguez-Fernández, C. Novo, V. Myroshnychenko, A.M. Funston, A. Sánchez-Iglesias, I. Pastoriza-Santos, J. Pérez-Juste, F.J. García de Abajo, L.M. Liz-Marzán, P. Mulvaney. Spectroscopy, imaging, and modeling of individual gold decahedra. *J. Phys. Chem. C*, 2009, vol. 113, no. 43, pp. 18623–18631.

[5] S. Choi, J.A. Herron, J. Scaranto, H. Huang, Y. Wang, X. Xia, T. Lv, J. Park, H. Peng, M. Mavrikakis, Y. Xia. A comprehensive study of formic acid oxidation on palladium nanocrystals with different types of facets and twin defects. *ChemCatChem*, 2015, vol. 7, no. 14, pp. 2077–2084.

[6] X. Wang, M. Vara, M. Luo, H. Huang, A. Ruditskiy, J. Park, S. Bao, J. Liu, J. Howe, M. Chi, Z. Xie, Y. Xia. Pd@Pt core–shell concave decahedra: a class of catalysts for the oxygen reduction reaction with enhanced activity and durability. *J. Am. Chem. Soc.*, 2015, vol. 137, no. 47, pp. 15036–15042.

[7] H. Huang, H. Jia, Z. Liu, P. Gao, J. Zhao, Z. Luo, J. Yang, J. Zeng. Understanding of strain effects in the electrochemical reduction of CO_2: using Pd nanostructures as an ideal platform. *Angew. Chemie*, 2017, vol. 129, no. 13, pp. 3648–3652.

[8] W. Zhu, A. Yin, Y. Zhang, C. Yan. Highly shape-selective synthesis of monodispersed fivefold twinned platinum nanodecahedrons and nanoicosahedrons. *Chem. Eur. J.*, 2012, vol. 18, no. 39, pp. 12222–12226.

[9] C.Y. Yang. Crystallography of decahedral and icosahedral particles. *J. Cryst. Growth*, 1979, vol. 47, no. 2, pp. 274–282.

[10] I.A. Polonsky, A.E. Romanov, V.G. Gryaznov, A.M. Kaprelov. Disclination in an elastic sphere. *Philos. Mag. A*, 1991, vol. 64, no. 2, pp. 281–287.

[11] A.E. Romanov, A.L. Kolesnikova. Elasticity boundary-value problems for straight wedge disclinations. A review on methods and results. *Rev. Adv. Mater. Technol.*, 2021, vol. 3, no. 1, pp. 55–95.

[12] R.E. Shevchuk, S.A. Krasnitckii, A.E. Romanov, A.M. Smirnov. Elasticity of pentagonal wires: single disclination model versus distributed disclination model. *Lett. Mater.*, 2024, vol. 14, no. 3, pp. 175–182.

[13] R.E. Shevchuk, S.A. Krasnitckii, A.M. Smirnov, A.E. Romanov. On the role of elastic anisotropy in the strain energy of decahedral metal particles: finite element analysis. *Contin. Mech. Thermodyn.*, 2026. [Submitted].

[14] A.P. Sutton. *Physics of Elasticity and Crystal Defects*. Oxford University Press, Oxford, 2024.

[15] W. Voigt. Ueber die beziehung zwischen den beiden elasticitätsconstanten isotroper körper. *Ann. Phys.*, 1889, vol. 274, no. 12, pp. 573–587. [In German].

[16] A. Reuss. Berechnung der fließgrenze von mischkristallen auf grund der plastizitätsbedingung für einkristalle. *Z. Angew. Math. Mech.*, 1929, vol. 9, no. 1, pp. 49–58. [In German].

[17] R. Hill. The elastic behaviour of a crystalline aggregate. *Proc. Phys. Soc. A*, 1952, vol. 65, no. 5, pp. 349–354.

[18] G. Simmons, H. Wang. *Single Crystal Elastic Constants and Calculated Aggregate Properties. A Handbook. Second Edition*. The MIT Press, Cambridge, Massachusetts, London, 1971.

[19] B.-J. Lee, J.-H. Shim, M.I. Baskes. Semiempirical atomic potentials for the fcc metals Cu, Ag, Au, Ni, Pd, Pt, Al, and Pb based on first and second nearest-neighbor modified embedded atom method. *Phys. Rev. B*, 2003, vol. 68, no. 14, art. no. 144112.

[20] S. Patala, L.D. Marks, M. Olvera de la Cruz. Elastic strain energy effects in faceted decahedral nanoparticles. *J. Phys. Chem. C*, 2013, vol. 117, no. 3, pp. 1485–1494.

УДК 539.3

Анизотропия и упругая энергия в декаэдрических частицах

А.М. Смирнов [1], Р.Э. Шевчук [1,2], С.А. Красницкий [1], А.Е. Романов [1,3]

[1] Университет ИТМО, Кронверкский пр., д. 49, лит. А, Санкт-Петербург, 197101, Россия
[2] Балтийский государственный технический университет «ВОЕНМЕХ» им. Д.Ф. Устинова, ул. 1-я Красноармейская, д. 1, Санкт-Петербург, 190005, Россия
[3] Физико-технический институт им. А.Ф. Иоффе РАН, ул. Политехническая, д. 26, Санкт-Петербург, 194021, Россия

Аннотация. В работе исследуется упругая энергия, запасённая в декаэдрических частицах (ДЧ), рассчитанная с помощью метода конечных элементов (КЭ), с учётом анизотропии материала частицы. Модель ДЧ состоит из пяти идеальных тетраэдров с геометрически необходимой щелью. Моделирование проводится в два этапа: на первом этапе происходит смыкание щели путём прикладывания необходимых перемещений к её краям, что приводит к появлению собственной деформации в частице; на втором этапе происходит упругая релаксация частицы с расчётом напряжённо-деформированного состояния. Для количественной оценки влияния анизотропии на упругие свойства частицы вводится коэффициент анизотропии с помощью инженерных упругих постоянных материала. Дано сравнение результатов численных расчётов с оценками изотропных аналитических моделей с применением трёх схем осреднения упругих постоянных: Фойгта, Рейсса и Хилла. Показано, что изотропное приближение завышает упругую энергию, причём схема Рейсса даёт наибольшее соответствие с КЭ решением (отклонения менее 26% даже для сильно анизотропного Pb). Для слабо анизотропных материалов, таких как Al, все три рассмотренные схемы дают близкие погрешности порядка 8%. Полученные результаты подчёркивают необходимость учёта анизотропии материала для точной количественной оценки упругой энергии в пентагональных частицах.

Ключевые слова: метод конечных элементов; запасенная упругая энергия; дисклинации; декаэдрические частицы